ACS APPLIED MATERIALS & INTERFACES

Letter

www.acsami.org

Beauty of Lotus is More than Skin Deep: Highly Buoyant Superhydrophobic Films

Yuri Choi,[†,‡] Teresa Brugarolas,[†] Sung-Min Kang,[§] Bum Jun Park,[†,∥] Byeong-Su Kim,[‡] Chang-Soo Lee,[§] and Daeyeon Lee*[,†]

[†]Department of Chemical and Biomolecular Engineering, University of Pennsylvania, Philadelphia, Pennsylvania 19104, United States

[‡]Department of Chemistry and Department of Energy Engineering, Ulsan National Institute of Science and Technology (UNIST), UNIST-gil 50, Ulsan 689-698, Korea

[§]Department of Chemical Engineering, Chungnam National University, Daejeon 305-764, Republic of Korea

[∥]Department of Chemical Engineering, Kyung Hee University, Yongin-si, Gyeonggi-do 446-701, Republic of Korea

Supporting Information

ABSTRACT: We develop highly buoyant superhydrophobic films that mimic the three-dimensional structure of lotus leaves. The high buoyancy of these structure stems from mechanically robust bubbles that significantly reduce the density of the superhydrophobic films. These highly buoyant superhydrophobic films stay afloat on water surface while carrying a load that is more than 200 times their own weight. In addition to imparting high buoyancy, the incorporation of robust hydrophilic bubbles enables the formation of free-standing structures that mimic the water-collection properties of Namib Desert beetle. We believe the incorporation of robust bubbles is a general method that opens up numerous possibilities in imparting high buoyancy to different structures that needs to stay afloat on water surfaces and can potentially be used for the fabrication of lightweight materials. (Image on the upper left reproduced with permission from Yong, J.; Yang, Q.; Chen, F.; Zhang, D.; Du, G.; Si, J.; Yun, F.; Hou, X. A Bioinspired Planar Superhydrophobic Microboat. *J. Micromech. Microeng.* **2014**, *24*, 035006. Copyright 2014 IOP Publishing.)

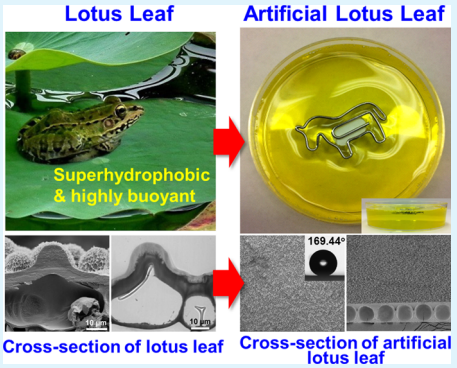

KEYWORDS: *superhydrophobicity, Lotus effect, bubbles, buoyancy, air sacs*

The extreme water repellency of lotus leaves, also known as superhydrophobicity, stems from the combination of low surface energy and hierarchical topology that are present on the leaf surface.[1,2] Water droplets roll freely on these leaf surfaces and remove dirt, keeping the leaves clean although many of these plants tend to grow in muddy waters.[2−4] This self-cleaning property, also known as the lotus effect, likely plays a critical role in the survival of the plant by keeping the surface clean and free of contamination and microoragnisms, and at the same time by facilitating efficient photosynthesis by allowing for direct exposure of the leaf surface to the sun light.

One crucial property of the lotus that has received relatively little attention, compared to its superhydrophobicity, is its high buoyancy. In fact, most reports mimicking the structure and functionality of the lotus have focused on emulating the topology and chemistry of these natural superhydrophobic surfaces.[5−18] Interestingly, the lotus has remarkable buoyancy and is able to stay afloat on the water surface even if a heavy creature such a frog or a bird sits on it. In fact, lotus leaves can easily support loads that are significantly heavier than their own weight. A typical frog, for example, can weigh a hundred times more than a single lotus leaf. Although superhydrophobic surfaces have a significant amount of air trapped between water and its surface, the buoyancy provided by this thin air layer is not sufficient to keep lotus leaves afloat under a heavy load.[19−21] This high buoyancy obviously is critical for the survival of the plant as submersion under water for an extended period of time could lead to the loss of superhydrophobicity, and hamper photosynthesis and gas exchange that are required to keep the plant alive.[2,22] The main reason for this excellent buoyancy is the presence of air chambers in the leaves of the lotus.[23] In fact, many types of aquatic plants also known as hydrophytes are known to have air sacs in their leaves, stems and roots making them highly buoyant in water.

In this work, we present the generation of a highly buoyant free-standing superhydrophobic structure. Inspired by the air sacs found in aquatic plants such as lotus, we impart high buoyancy to free-standing superhydrophobic films by embedding nanoparticle-shelled bubbles in the structure. These highly buoyant structures are able to stay afloat on water surface even if a heavy object (more than 200 times heavier than the structure itself) is placed on them. In addition to generating highly buoyant superhydrophobic surfaces, we also show that highly buoyant surfaces that emulate the water collection

Received: March 14, 2014
Accepted: May 6, 2014
Published: May 6, 2014

   dx.doi.org/10.1021/am5015343 | *ACS Appl. Mater. Interfaces* 2014, 6, 7009−7013

properties of the Namib Desert beetle can be generated by tailoring the fabrication procedure.[24,25]

A highly buoyant structure with extreme wettability is generated by incorporating mechanically robust hollow shells (or bubbles) into a free-standing superhydrophobic film as illustrated in Scheme 1. The first step of this process involves

Scheme 1. (A) Schematic Illustration of Highly Buoyant Superhydrophobic Composite Containing Nanoparticle-Shelled Bubbles; (B) Cross-Sectional SEM and (C) Optical Microscopy Images of Lotus Leaves Showing Air Sacs; Reproduced with Permission from Ref 2 2011, Beilstein Journals

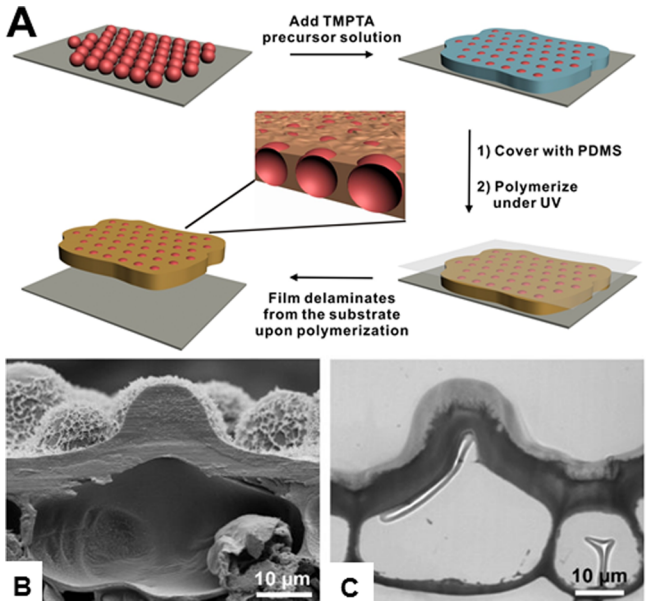

the generation of highly stable bubbles, which we accomplish using a microfluidic method. In our previous study, we demonstrated that highly robust nanoparticle-shelled bubbles can be generated by using microfluidic gas-in-oil-in-water (G/O/W) compound bubbles as templates.[26−28] Hydrophobic silica nanoparticles are suspended in the oil phase of G/O/W compound bubbles and subsequently form the shell of the bubbles after the solvent (toluene) is removed from the oil phase via evaporation. The stiff shell generated at the air−water interface prevents the dissolution of the gas in the core and keeps these bubbles stable for an indefinite period of time. These nanoparticle-shelled bubbles are dried on a surface to form a hexagonally arranged monolayer without any degradation of their structure and properties (especially, their buoyancy). Bubbles arrange themselves into a hexagonal array at the air−water interface of a sessile drop because of their high monodispersity and maintain their arrangement on the surface even after water evaporates.[26] It is critical to keep the ratio of the shell thickness and bubble radius above a critical value (~0.042) to prevent the collapsing of bubbles, as reported in the prior work.[26]

A free-standing superhydrophobic composite film containing this bubble monolayer is generated using a recently developed superhydrophobic preparation method.[29] It was shown that when a monomer mixture containing trimethylolpropane triacrylate (TMPTA) and lauryl acrylate (LA) (9:1 v/v) in ethanol is covered with a polydimethylsiloxane (PDMS) slab and subsequently photopolymerized under UV irradiation, a superhydrophobic surface with high surface roughness is generated. The wettability of the surface depends on the concentration of ethanol in the precursor solution; superhydrophobic surfaces are generated when the concentration of ethanol is over 50% (see Figure S1 in the Supporting Information). The hysteresis between the receding and advancing contact angles on the polymerized TMPTA/LA film from the precursor solution with more than 50% ethanol is less than 5°, illustrating excellent superhydrophobicity. It is believed that Marangoni stress developed during the photopolymerization under PDMS as well as the surface segregation of the more hydrophobic monomer, LA, to the PDMS/precursor solution interface, leads to highly rough and superhydrophobic surfaces from the mixture of TMPTA and LA. The mechanism behind the formation of superhydrophobic structure and the role of PDMS cover during photopolymerization has been discussed more in detail elsewhere.[29]

To form a highly buoyant superhydrophobic structure, we dispense a drop of the TMPTA/LA mixture in ethanol (monomer mixture:ethanol = 1:10 in volumetric ratio) over a dried bubble monolayer. Because of the capillarity, the solution readily wicks into the interstices between the bubbles and stays within the interstices. The sample is subsequently covered with a slab of PDMS and polymerized under UV irradiation. The precursor solution turns opaque upon polymerization, indicating the formation of highly porous and rough structure. Also the polymerized structure delaminates from the glass substrate, likely because of the stress build-up within the film during polymerization and weak adhesion between the polymer and the glass substrate.

The topology as well as the wettability of these bubble-containing free-standing composite films could be readily controlled by adding different amounts of the precursor solution prior to photopolymerization. When 20 μL of the precursor solution is placed over a bubble monolayer that is approximately 1.5 cm in diameter and subsequently polymerized under UV illumination, the resulting structure exposes the top portion of the embedded bubbles as shown in Figure 1A. Increasing the amount of the precursor solution leads to complete coverage of the bubbles as shown in Figure 1B and C. It is important to note that the surface of the nanoparticle-shelled bubbles is relatively hydrophilic (contact angle ~65°) due to the presence of poly(vinyl alcohol) (PVA) that is used to stabilize G/O/W compound bubbles during their microfluidic generation.[26] Accordingly, the wettability of the composite structure becomes more hydrophobic as the amount of the precursor solution is increased (Figure 1H). The contact and sliding angles of the composite sample with 80 μL of the precursor solution exhibited essentially the same values (contact angle ~170°; sliding angle <5°) as those of the neat TMPTA/LA mixture polymerized without nanoparticle-shelled bubbles (Figure 1H). In all cases, the shape of embedded bubbles is not significantly deformed from their original spherical shape, and no polymer is found in the interior of the bubbles as seen in the cross-section SEM images in Figure 1. These bubbles embedded in the bulk of the composite films (Figure 1B, D and F) indeed resemble the air sacs found in the cross-section image of lotus leaves shown in Scheme 1. The density of a superhydrophobic film without nanoparticle-shelled bubbles, determined by directly measuring its volume and mass, is ~1.3 g/cm^3, whereas the density of a superhydrophobic film with nanoparticle-shelled bubbles is significantly lower at ~0.4 g/cm^3 because of the presence of the air

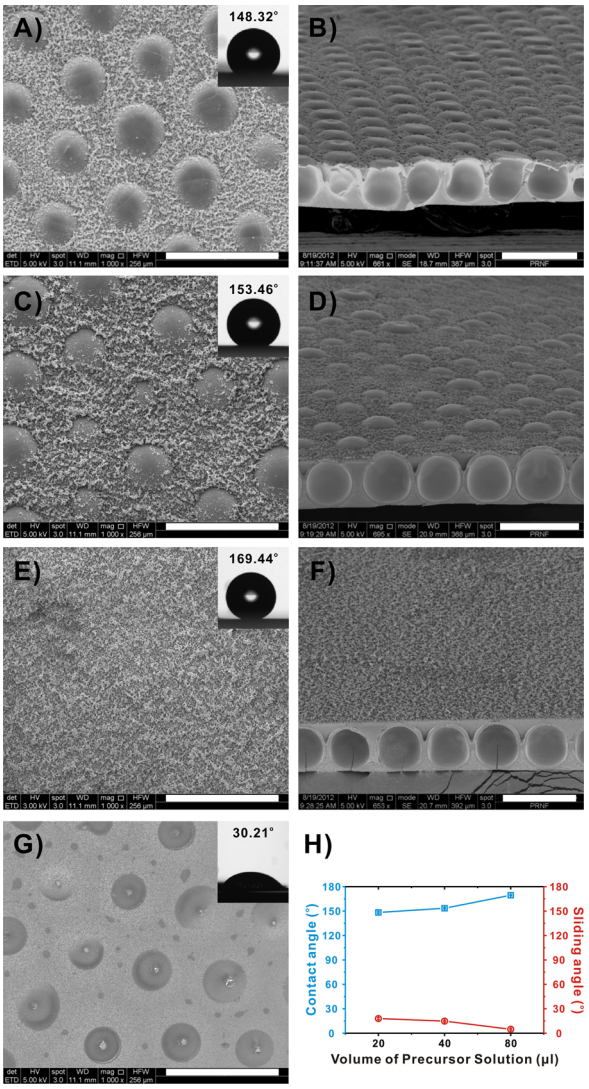

Figure 1. Geometry and surface properties controlled by the thickness of TMPTA polymer layer. (A, B) Beetlelike structure in which the microbubbles are partially exposed (20 μL of precursor solution). SEM images of (A) the superhydrophobic bumpy surface and (B) the cross-sectional structure. (C, D) Beetlelike structure in which the bubbles are partially exposed from the polymer layer (40 μL of precursor solution). SEM images of (C) superhydrophobic top-surface, and (D) cross-sectional structure. (E, F) Lotuslike structure in which the entire bubbles are immersed in the polymer layer (80 μL of precursor solution). SEM images of (E) superhydrophobic top-surface, and (F) cross-sectional structure. (G) SEM image of the hydrophilic bottom surface. Insets in panels A, C, E, and G indicate the corresponding contact angle of a water droplet on the each surface. (H) Contact angle and sliding angle depending on the thickness of TMPTA polymer layer. The scale bars are 100 μm. The slide angle is the tilt angle of the surface at which a water droplet freely slides on the surface.

sacs (see the Supporting Information). The low density of bubble-containing films likely will play an important role in imparting high buoyancy to these structures.

Interestingly, the wettability of the bottom side of the free-standing composites (i.e., the side that was in contact with the glass slide) is found to be quite hydrophilic, imparting amphiphilicity to the free-standing structure. The contact angle of the bottom side is found to be approximately 30° as shown in the inset of Figure 1G. This surprising result is consistent with a recent report, which showed that when the photopolymerization of the TMPTA/LA mixture is performed under a glass cover (rather than a PDMS slab),[29] the polymerized TMPTA/LA surface is indeed hydrophilic. The absence of surface roughness (Figure 1G) and likely the surface segregation of the more hydrophilic monomer, TMPTA, to the precursor/glass interface lead to the formation of the hydrophilic surface. We find that the amphiphilicity of the free-standing composite films is quite advantageous as it makes the placement of the free-standing composite films on the water surface straightforward as the hydrophilic side readily spreads on the water surface, nicely exposing the superhydrophobic side to air.

The surface wetting properties of the bubble-containing free-standing composite films depend significantly on the topology of the structure. When the bubbles are completely covered by the rough structure of the photopolymerized TMPTA/LA mixture, the behavior of water droplets on these surfaces is essentially identical to that of water droplets on the bubble-free superhydrophobic surfaces. Water droplets are able to bounce and roll off the tilted surface (~20°) with ease as would be expected for superhydrophobic surfaces (Figure 2C).

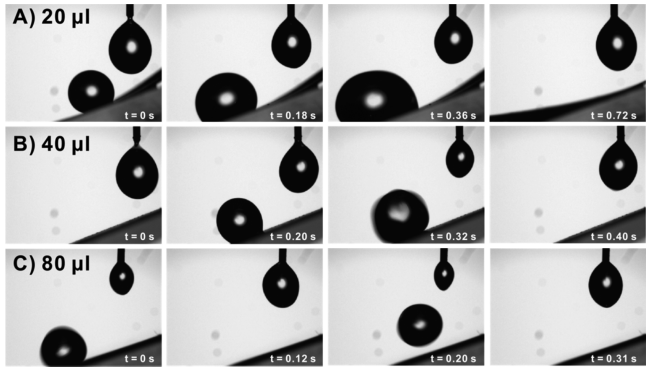

Figure 2. Snapshots of water droplets rolling on tilted superhydrophobic surfaces. (A, B) Beetlelike structure in which the microbubbles partially protrude to the surface of the polymer layer; (A) 20 μL and (B) 40 μL of precursor solution are used. (C) Lotus-leaf-like structure in which the entire bubbles are immersed in the polymer layer (80 μL of precursor solution). See the Supporting Information for movies.

When the bubbles are partially exposed because of an insufficient amount of the TMPTA/LA precursor solution, partially exposed bubbles form hexagonal arrays of hydrophilic patches surrounded by a superhydrophobic background. Such a surface is reminiscent of the unique structure found on the back of the Namib Desert beetle, stenocara gracilipes.[24,25] These beetles are known to capture water on its bumpy back surface from early morning fog. The back of the Namib Desert beetle is composed of hydrophilic bumps on a hydrophobic surface. It has been shown that water droplets in the morning fog collect and stay pinned on the hydrophilic bumps. When the water droplets become very large, droplets are able to detach themselves from the hydrophilic patches and freely roll on the superhydrophobic surface and reach the mouth of the beetles.

Similar to the water collecting surfaces of the Namib Desert beetle, when water droplets are placed on the slightly tilted bubble-exposing surfaces, they initially stay pinned on the surface likely due to the exposed bubble surface that is

dx.doi.org/10.1021/am5015343 | ACS Appl. Mater. Interfaces 2014, 6, 7009−7013

hydrophilic as shown in photo groups A and B in Figure 2. As water droplets (approximately 3 μL) are continuously added to the surface, the size of the pinned water droplet grows until the gravitational force enables the water droplet to overcome the pinning on the surface and to roll off the surface. The size of the water droplets that stay pinned increases with the area of the exposed bubble surface. This simple demonstration illustrates the versatility of our method in controlling the wetting properties and possibly imparting water collection capability to these bubble-containing structures.

These bubble-containing superhydrophobic composite films are significantly more buoyant than their counterparts without any bubbles. To demonstrate their high buoyancy, we generate two superhydrophobic films that have approximately the same area; one sample has bubbles embedded in the film, whereas the other one does not. When placed on the water surface, both of these samples are able to sustain their own weight and stay afloat. Also, the samples remain superhydrophobic as seen in Figure 3A. However, when we place an object that is

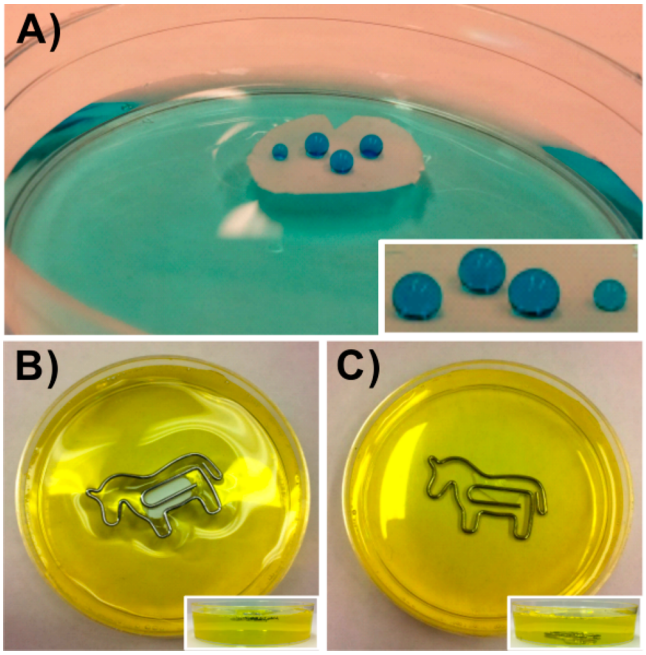

Figure 3. (A) Snapshot of the composite film (1.5 × 1.5 cm^2) floating at the air−water interface. Water droplets are placed on the top of the superhydrophobic surface. (B) Composite film (80 μL of precursor solution was used to make the free-standing film) containing nanoparticle-shelled bubbles show enhanced buoyancy resisting a significant amount of load (~230 times heavier than the composite film), whereas (C) the superhydrophobic polymer film without bubbles sinks upon placing the load on top of the sample.

approximately 230 times heavier than the weight of the free-standing films, the superhydrophobic film without bubbles sinks instantly to the bottom of the container (Figure 3C), whereas the one with the bubbles (air sacs) is able to stay afloat indefinitely as seen in Figure 3B. These results clearly indicate that the superhydrophobicity of the film, thus surface tension force, alone does not impart significant buoyancy to the structure and that it is critical to have nanoparticle-shelled bubbles in the film to impart substantial buoyancy. This high buoyancy, of course, can be attributed to the bubbles that are embedded within the bulk of the sample. To our best knowledge, we believe this is the first example of air sac-containing superhydrophobic structure that mimics the three-dimensional structure and high buoyancy of the lotus and many other aquatic plants. Detailed analysis of the deformation of air−water interface around superhydrophobic films could potentially distinguish the relative importance of surface tension forces and material density in imparting high buoyancy in these bubble-containing superhydrophobic films.[30,31]

We report the generation of a highly buoyant lotus-leaf-like composite structure by embedding robust nanoparticle-shelled bubbles in a superhydrophobic structure. Bubble-containing superhydrophobic composite films show exceptional buoyancy that cannot be readily achieved by typical superhydrophobic surfaces. We also show that by controlling the exposure of the bubbles at the surface of the composite, either superhydrophobic or water-collecting surfaces can be generated. We believe the incorporation of robust bubbles is a general method that opens up numerous possibilities in imparting high buoyancy to different structures that needs to stay afloat on water surfaces and can potentially be used for the fabrication of lightweight materials.

■ ASSOCIATED CONTENT

Supporting Information

Experimental details, movies showing water droplets sliding on the superhydrophobic surfaces, and characterization of superhydrophobic films. This material is available free of charge via the Internet at http://pubs.acs.org.

■ AUTHOR INFORMATION

Corresponding Author

*E-mail: daeyeon@seas.upenn.edu.

Notes

The authors declare no competing financial interest.

■ ACKNOWLEDGMENTS

This work was primarily supported by a NSF CAREER Award (DMR-1055594) and partly by the Penn MRSEC (NSF-1120901). Y.C. was supported by the BK21 Plus funded by the Ministry of Education, Korea (10Z20130011057). T.B. acknowledges the graduate fellowship from Obra Social "La Caixa".

■ REFERENCES

(1) Barthlott, W.; Neinhuis, C. Purity of the Sacred Lotus, or Escape from Contamination in Biological Surfaces. *Planta* **1997**, *202*, 1−8.
(2) Ensikat, H. J.; Ditsche-Kuru, P.; Neinhuis, C.; Barthlott, W. Superhydrophobicity in Perfection: The Outstanding Properties of the Lotus Leaf. *Beilstein J. Nanotechnol.* **2011**, *2*, 152−161.
(3) Blossey, R. Self-Cleaning Surfaces—Virtual Realities. *Nat. Mater.* **2003**, *2*, 301−306.
(4) Choi, C. H.; Kim, C. J. Large Slip of Aqueous Liquid Flow over a Nanoengineered Superhydrophobic Surface. *Phys. Rev. Lett.* **2006**, *96*, 066001.
(5) Feng, X. J.; Jiang, L. Design and Creation of Superwetting/Antiwetting Surfaces. *Adv. Mater.* **2006**, *18*, 3063−3078.
(6) Liu, M. J.; Wang, S. T.; Jiang, L. Bioinspired Multiscale Surfaces with Special Wettability. *MRS Bull.* **2013**, *38*, 375−382.
(7) Wang, S.; Jiang, L. Definition of Superhydrophobic States. *Adv. Mater.* **2007**, *19*, 3423−3424.
(8) Zhai, L.; Cebeci, F. C.; Cohen, R. E.; Rubner, M. F. Stable Superhydrophobic Coatings from Polyelectrolyte Multilayers. *Nano Lett.* **2004**, *4*, 1349−1353.
(9) Jeong, C. Y.; Choi, C. H. Single-Step Direct Fabrication of Pillar-on-Pore Hybrid Nanostructures in Anodizing Aluminum for Superior

Superhydrophobic Efficiency. *ACS Appl. Mater. Interfaces* **2012**, *4*, 842−848.
(10) Nakajima, A.; Hashimoto, K.; Watanabe, T. Recent Studies on Super-Hydrophobic Films. *Monatsh. Chem.* **2001**, *132*, 31−41.
(11) Onda, T.; Shibuichi, S.; Satoh, N.; Tsujii, K. Super-Water-Repellent Fractal Surfaces. *Langmuir* **1996**, *12*, 2125−2127.
(12) Oner, D.; McCarthy, T. J. Ultrahydrophobic Surfaces. Effects of Topography Length Scales on Wettability. *Langmuir* **2000**, *16*, 7777−7782.
(13) Roach, P.; Shirtcliffe, N. J.; Newton, M. I. Progess in Superhydrophobic Surface Development. *Soft Matter* **2008**, *4*, 224−240.
(14) Tuteja, A.; Choi, W.; Ma, M. L.; Mabry, J. M.; Mazzella, S. A.; Rutledge, G. C.; McKinley, G. H.; Cohen, R. E. Designing Superoleophobic Surfaces. *Science* **2007**, *318*, 1618−1622.
(15) Sun, T. L.; Feng, L.; Gao, X. F.; Jiang, L. Bioinspired Surfaces with Special Wettability. *Acc. Chem. Res.* **2005**, *38*, 644−652.
(16) Li, X. M.; Reinhoudt, D.; Crego-Calama, M. What Do We Need for a Superhydrophobic Surface? A Review on the Recent Progress in the Preparation of Superhydrophobic Surfaces. *Chem. Soc. Rev.* **2007**, *36*, 1350−1368.
(17) Nosonovsky, M.; Bhushan, B. Superhydrophobic Surfaces and Emerging Applications: Non-Adhesion, Energy, Green Engineering. *Curr. Opin. Colloid Interface Sci.* **2009**, *14*, 270−280.
(18) Celia, E.; Darmanin, T.; de Givenchy, E. T.; Amigoni, S.; Guittard, F. Recent Advances in Designing Superhydrophobic Surfaces. *J. Colloid Interface Sci.* **2013**, *402*, 1−18.
(19) Lee, C.; Kim, C. J. Underwater Restoration and Retention of Gases on Superhydrophobic Surfaces for Drag Reduction. *Phys. Rev. Lett.* **2011**, *106*, 014502.
(20) Pan, Q. M.; Liu, J.; Zhu, Q. A Water Strider-Like Model with Large and Stable Loading Capacity Fabricated from Superhydrophobic Copper Foils. *ACS Appl. Mater. Interfaces* **2010**, *2*, 2026−2030.
(21) Su, Y. W.; Ji, B. H.; Huang, Y.; Hwang, K. C. Nature's Design of Hierarchical Superhydrophobic Surfaces of a Water Strider for Low Adhesion and Low-Energy Dissipation. *Langmuir* **2010**, *26*, 18926−18937.
(22) Zhang, J. H.; Sheng, X. L.; Jiang, L. The Dewetting Properties of Lotus Leaves. *Langmuir* **2009**, *25*, 1371−1376.
(23) Hodson, M. J.; Braynt, J. A. *Functional Biology of Plants*; Wiley-Blackwell: Hoboken, NJ, 2012.
(24) Zhai, L.; Berg, M. C.; Cebeci, F. C.; Kim, Y.; Milwid, J. M.; Rubner, M. F.; Cohen, R. E. Patterned Superhydrophobic Surfaces: Toward a Synthetic Mimic of the Namib Desert Beetle. *Nano Lett.* **2006**, *6*, 1213−1217.
(25) Parker, A. R.; Lawrence, C. R. Water Capture by a Desert Beetle. *Nature* **2001**, *414*, 33−34.
(26) Brugarolas, T.; Park, B. J.; Lee, M. H.; Lee, D. Generation of Amphiphilic Janus Bubbles and Their Behavior at an Air-Water Interface. *Adv. Funct. Mater.* **2011**, *21*, 3924−3931.
(27) Lee, M. H.; Lee, D. Elastic Instability of Polymer-Shelled Bubbles formed from Air-in-Oil-in-Water Compound Bubbles. *Soft Matter* **2010**, *6*, 4326−4330.
(28) Lee, M. H.; Prasad, V.; Lee, D. Microfluidic Fabrication of Stable Nanoparticle-Shelled Bubbles. *Langmuir* **2010**, *26*, 2227−2230.
(29) Kang, S.-M.; Hwang, S.; Jin, S. H.; Choi, C.-H.; Kim, J.; Park, B. J.; Lee, D.; Lee, C.-H. A Rapid One-Step Fabrixation of Patternable Superhydrophobic Surfaces Driven by Marangoni Instability. *Langmuir* **2014**, *30*, 2828−2834.
(30) Extrand, C. W.; Moon, S. I. Will It Float? Using Cylindrical Disks and Rods to Measure and Model Capillary Forces. *Langmuir* **2009**, *25*, 2865−2868.
(31) Extrand, C. W.; Moon, S. I. Using the Floatation of a Single Sphere to Measure and Model Capillary Forces. *Langmuir* **2009**, *25*, 6239−6244.